Solid-State ^{13}C NMR of Poly(butylene terephthalate)/Polyarylate Blends

Peter P. Huo† and Peggy Cebe*

Department of Materials Science and Engineering, Massachusetts Institute of Technology, Cambridge, Massachusetts 02139

Received April 27, 1993; Revised Manuscript Received July 13, 1993®

ABSTRACT: Miscible blends of poly(butylene terephthalate) (PBT) with polyarylate (PAr) have been investigated by solid-state ^{13}C NMR. High-resolution solid-state NMR results show that the chemical shifts of PBT and PAr in the PBT/PAr blends have the same values as their homopolymer counterparts. The proton relaxation times in the rotating frame have been measured through the proton–carbon cross-polarization study. Results indicate that the $T_{1\rho}^{H}$ for quenched PBT and PAr are very close in value, at 2.5 and 2.8 ms, respectively. For the melt-crystallized PBT and PBT/PAr blends, the NMR line width decreases as the PAr content increases, indicating more perfect crystals appear in the blends compared with that in the PBT homopolymer. This is a result of the much slower crystallization of PBT in the blends. Protonated aromatic carbons of PBT in melt-crystallized PBT and PBT/PAr blends for the first time are shown to exhibit peak splitting, due to chain conformation effects.

1. Introduction

Blends of poly(butylene terephthalate) (PBT) with polyarylate (PAr) have been shown to be miscible at all compositions in the melt or in the amorphous state.[1-6] This is based on the measurement of the glass transition by using differential scanning calorimetry (DSC),[1] dynamic mechanical analysis (DMA),[6] and dielectric relaxation spectroscopy.[2] Our previous results on the equilibrium melting point depression of PBT in the PBT/PAr blends lead to the conclusion of a negative interaction parameter.[5] Both quenched and crystallized PBT/PAr blends have been investigated by dynamic mechanical analysis and small-angle X-ray scattering.[6] Results indicate that crystallized blends with a PAr mass function less than 0.40 exhibit an interlamellar structure, and blends with a PAr mass fraction higher than 0.40 possess an interfibrillar or interspherulitic structure. The purpose of our previous studies is to investigate the effect of PAr on PBT for both quenched and crystallized blends in terms of the morphological aspects.

There have been extensive reports of the solid-state ^{13}C NMR studies of PBT homopolymer.[7-11] Both carbon-13[7-10] and deuterium[11] NMR were used to explore the conformation, the relaxation, and the local motion of PBT. But, so far, there are no studies of PBT/PAr blends using solid-state ^{13}C NMR, although solution proton NMR was used to investigate the transesterification reaction for PBT/PAr blends.[12] To compliment our prior thermal, dynamic mechanical, and small-angle X-ray scattering studies[5,6] and to access information at the molecular level, we present here results of our ^{13}C NMR spectroscopy study of PBT/PAr blends prepared over a wide composition range. Dipolar decoupling, magic angle spinning, and cross-polarization techniques were performed to obtain the high-resolution ^{13}C-NMR spectra of quenched and melt-crystallized PBT, PAr, and PBT/PAr blends. One of the main observations of this work is the splitting of the ortho carbons in the terephthalate rings of well-crystallized blends which is due to chain conformation effects.

† Present address: Analytical Division, W. R. Grace Corp., Columbia, MD 21045.

® Abstract published in *Advance ACS Abstracts*, September 1, 1993.

2. Experimental Section

Poly(butylene terephthalate) was obtained from Polysciences. Polyarylate was obtained from Amoco, with a 1:1 ratio of isophthalic and terephthalic units. Blends of PBT/PAr weight fractions 80/20, 60/40, 40/60, and 20/80 were made by following the method of Kimura et al.,[1] which involves coprecipitation from phenol/TCE into methanol. The quenched samples were made by heating the precipitates to 250 °C, holding for 60–90 s, compression molding, and then quenched in ice water. The quenched PBT and 80/20 blend show a little paracrystallinity, while quenched 60/40, 40/60, and 20/80 blends are purely amorphous. Melt-crystallized samples were prepared by heating the quenched film from room temperature to 250 °C for 1 min using a Mettler FP80 hot stage, then cooling quickly to the crystallization temperature T_c, and holding there for a time sufficient for completion of crystallization as required by the crystallization kinetics.[3] Crystallized samples prepared in the above way possess only α-form crystals as investigated by wide-angle X-ray scattering.[14-16]

Furthermore, we used differential scanning calorimetry in a cyclic procedure to test the transesterification reaction at 250 °C. A previous report by Kimura et al. indicates that the transesterification reaction is severe only after holding at 250 °C for more than 100 min.[1] To test this, we scanned the 60/40 blend at 20 °C/min 10 times from room temperature to 250 °C and held there for times ranging from 2 to 30 min. The DSC scans were the same for accumulated times shorter than 10 min but show significant differences as the total time at 250 °C approached 1 h. This indicates that the blend sample we prepared for 1 min at 250 °C has not undergone any transesterification reaction.

High-resolution solid-state ^{13}C NMR spectra were measured using an IBM NR/200 AF (4.7 T) spectrometer operating at 50.3 MHz fitted with an IBM solid accessory rack which housed the high-power amplifier and Doty Scientific probe for magic angle spinning. Contact time dependences of spectra for both homopolymers and blends were performed by varying the contact time from 50 to 1000 μs. A contact time of 1000 μs was found to be the best for all carbons for both homopolymers and blends. Dipolar decoupling was used in conjunction with a cross-polarization pulse sequence employing a 5-μs proton 90° pulse, a 1-ms contact time, and a 3-s recycle delay. Solid-state spectra were referenced to the methyl resonance of *p*-di-*tert*-butylbenzene (31.0 ppm from TMS).

3. Results and Discussion

For cross-polarization techniques, contact time is one of the most important parameters. Due to the different

0024-9297/93/2226-5561$04.00/0

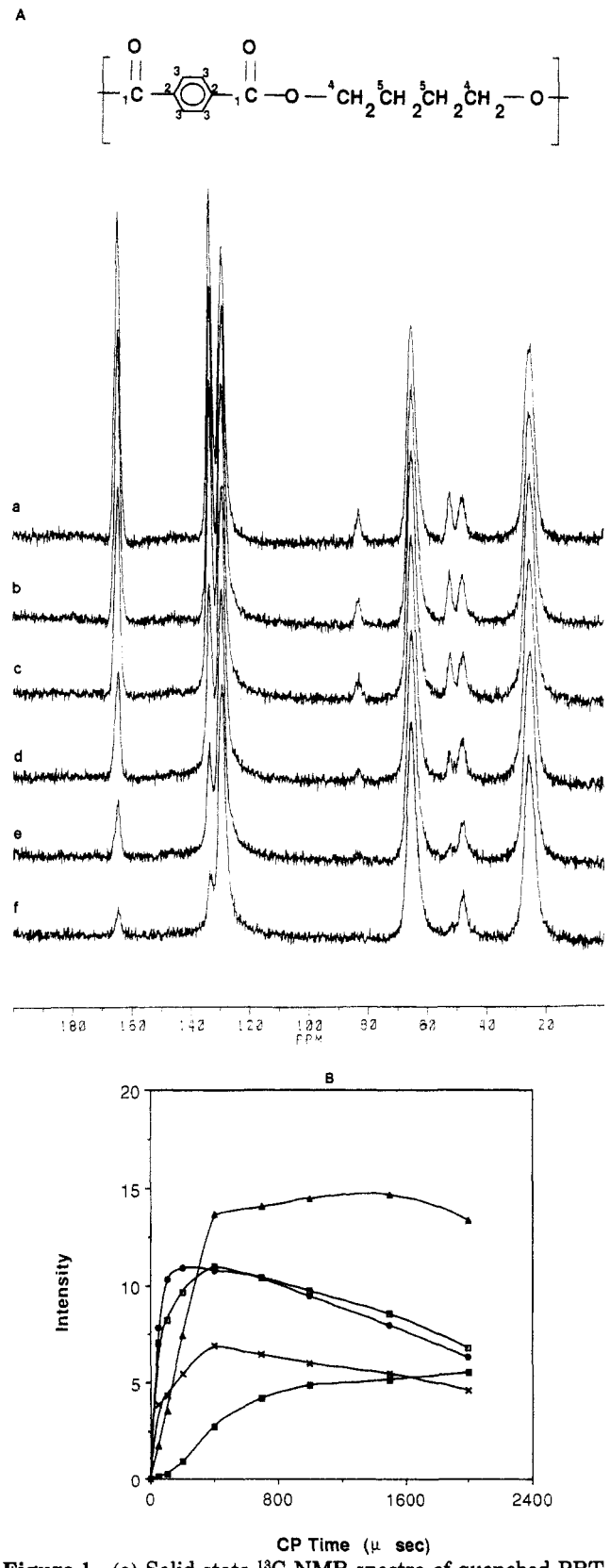

Figure 1. (a) Solid-state ^{13}C NMR spectra of quenched PBT for contact times of (a) 1000, (b) 700, (c) 400, (d) 200, (e) 100, and (f) 50 μs. (b) Peak intensities for quenched PBT as a function of cross-polarization time: carbon 1 (■), carbon 2 (▲), carbon 3 (×), carbon 4 (⊡), carbon 5 (●). The chemical structure is shown at the top of A, with carbons numbered from highest to lowest chemical shift.

efficiency of cross polarization between different carbons and protons, we therefore expect that the NMR spectrum, and more specifically the relative peak intensity, will be dependent on the contact time. The contact time dependence of quenched PBT is shown in Figure 1a which shows the peak profile vs chemical shift for contact times ranging from 50 to 1000 μs. The peak intensity for the five peaks of quenched PBT vs contact time is presented in Figure 1b. At the top of Figure 1a the chemical structure of PBT is shown with carbons numbered. There exist five peaks numbered from highest to lowest chemical shift: (1) the carbonyl (C=O), (2) nonprotonated aromatic (NPA), (3) protonated aromatic (PA), (4) exterior methylenes (OCH_2), and (5) interior methylenes (CH_2). The chemical shifts of each of the different carbons are listed as follows:

chemical shifts of PBT in ppm

(1) 164.2 (2) 133.5 (3) 129.1 (4) 64.8 (5) 24.7

The agreement of the chemical shift is excellent compared with the previous results on homopolymer PBT.[7-10] As can be seen from parts a and b of Figure 1, aliphatic (both exterior and interior methylenes) and protonated aromatic carbon resonance peaks increase quickly, showing almost the strongest intensity at a contact time equal to 50 μs. Both nonprotonated and carbonyl carbon peak intensities are weak at 50 μs, and they increase slowly as contact time increases. At contact time 500–1000 μs, all peaks appear to be at about their maximum values, although the two aliphatic peaks start to decline as the contact time increases above 500 μs. This decline is due to the relaxation of protons in their rotating frame, which occurs with a time constant, $T_{1\rho}^{H}$, the proton spin–lattice relaxation time in the rotating frame.

In parts a and b of Figure 2, we present the contact time dependence of PAr NMR spectra and peak intensity, respectively. The PAr chemical structure is shown at the top of Figure 2A with the carbons numbered. For PAr, we observed eight peaks, assigned to their corresponding carbons as shown at the top of Figure 2A, numbered from highest to lowest chemical shift. The chemical shifts of these eight peaks are listed as follows:

chemical shifts of PAr in ppm

(1) 163.2 (2) 148.2 (3) 133.6 (4) 129.5
(5) 127.0 (6) 120.3 (7) 41.6 (8) 29.9

The carbonyl carbon (PAr 1) and nonprotonated carbon (PAr 3) peak intensities appear to be small at short contact time, similar to that of PBT, and increase slowly as contact time increases. The protonated aromatic carbon (PAr 4) peak intensity increases quickly and then decreases as the contact time increases above 400 μs. The same study has been performed on quenched PBT/PAr blends, indicating a similar behavior for the growth of peaks as a function of contact time compared to the homopolymers.

The contact time dependence of peak intensity can be expressed by the following relationship developed previously:[17]

$$M(t) = A[1 - \exp(-\lambda t/T_{CH})] \exp(-t/T_{1\rho}^{H}) \quad (1)$$

where λ is defined as:

$$\lambda = 1 + \left(\frac{T_{CH}}{T_{1\rho}^{C}} - \frac{T_{CH}}{T_{1\rho}^{H}}\right) \quad (2)$$

where t is the H–C spin-lock time (which is the variable), T_{CH} is the cross-polarization time, which is dependent on the specific carbons under investigation, and $T_{1\rho}^{H}$ and $T_{1\rho}^{C}$ are the proton and carbon spin–lattice relaxation times in the rotating frame. $T_{1\rho}^{H}$ is the same for each carbon due to the strong spin diffusion, while $T_{1\rho}^{C}$ is different for different carbons. For polymers, $T_{1\rho}^{C} \gg T_{1\rho}^{H}$.

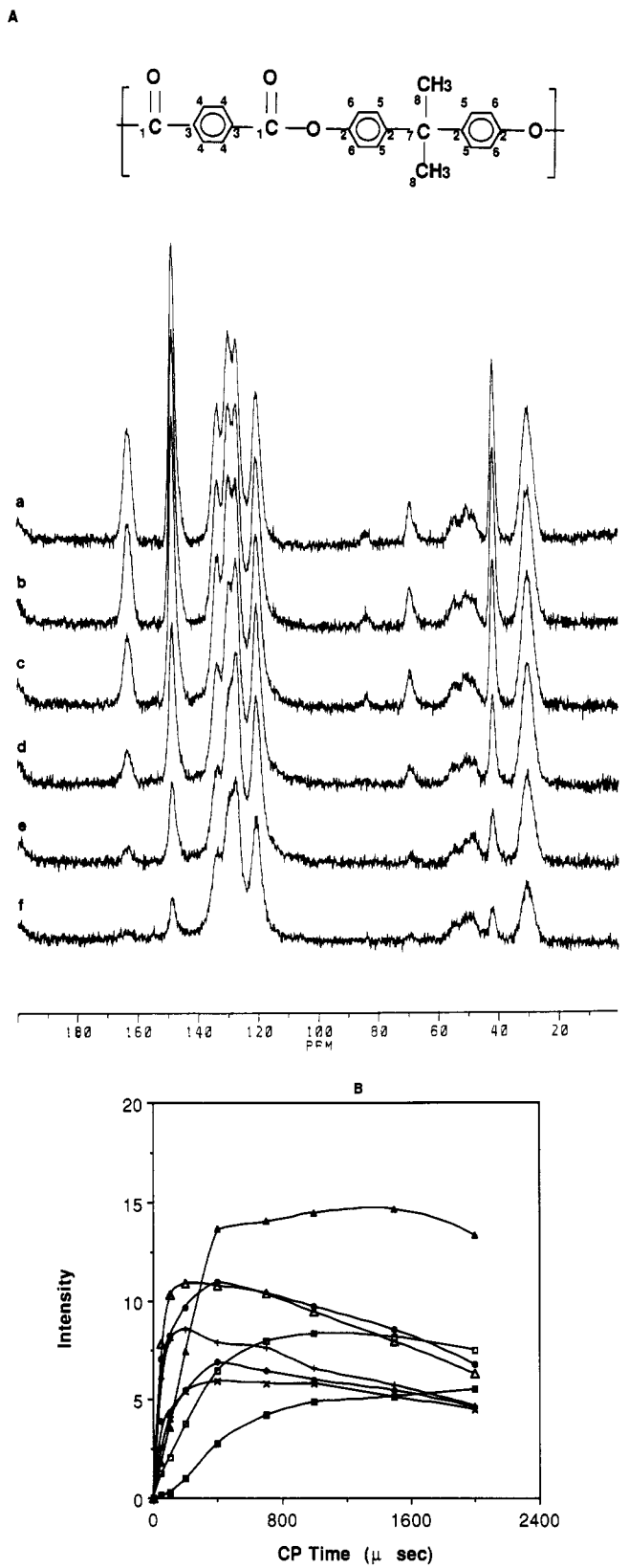

Figure 2. (a) Solid-state ^{13}C NMR spectra of PAr for contact times as listed in Figure 1A. (b) Peak intensities for PAr as a function of cross-polarization time: carbon 1 (■), carbon 2 (▲), carbon 3 (◆), carbon 4 (●), carbon 5 (△), carbon 6 (+), carbon 7 (□), carbon 8 (×). The chemical structure is shown at the top of A, with carbons numbered from highest to lowest chemical shift.

Then $\lambda = 1 - T_{CH}/T_{1\rho}^{H}$, and $M(t)$ evolves to the following:[17]

$$M(t) = A[\exp(-t/T_{1\rho}^{H}) - \exp(-t/T_{CH})] \quad (3)$$

For those peaks that have $T_{1\rho}^{H} \gg T_{CH}$, the second term of eq 3 vanishes at long contact time. We therefore can use the long contact time portion of the data from those peaks to obtain the value of $T_{1\rho}^{H}$. Due to the extremely strong proton spin diffusion, $T_{1\rho}^{H}$ is nearly the same for each sample, independent of the specific carbons used for the calculation of $T_{1\rho}^{H}$. The quenched PBT has $T_{1\rho}^{H}$ = 2.5 ms, while PAr has $T_{1\rho}^{H}$ = 2.8 ms. For polymer blends, we observe either two $T_{1\rho}^{H}$ or a single $T_{1\rho}^{H}$, all of which are between the $T_{1\rho}^{H}$ of the two homopolymers. Generally, if a single $T_{1\rho}^{H}$ is observed, a blend miscible within a certain length scale is assumed, while an immiscible blend is assumed if two $T_{1\rho}^{H}$ are measured. The above method is only valid for those blends that have very different $T_{1\rho}^{H}$ values for the two homopolymers. Here, the $T_{1\rho}^{H}$ for PBT and PAr are very close, and therefore a miscibility study via $T_{1\rho}^{H}$ measurement is not feasible under the condition of our experiment.[17]

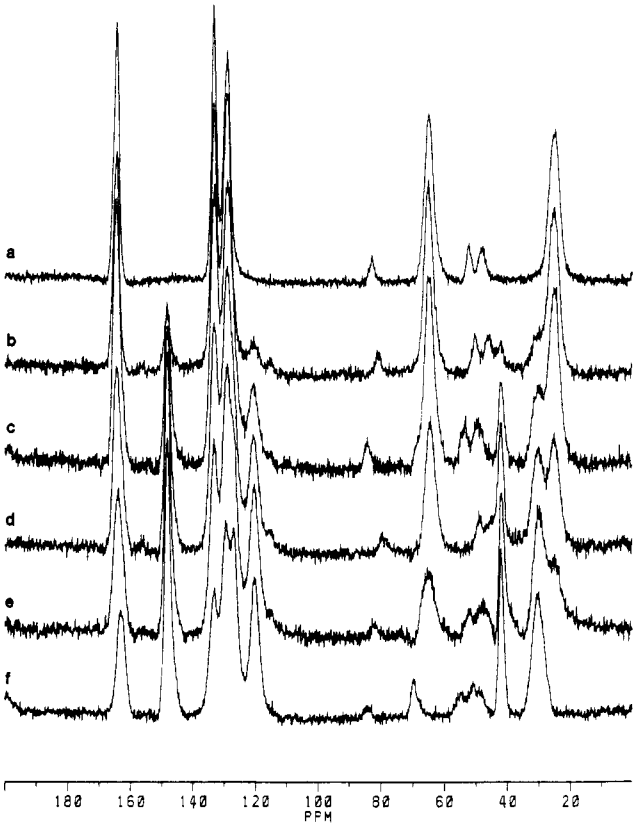

Figure 3. Solid-state ^{13}C NMR spectra for quenched PBT/PAr blends at a cross-polarization time of 1000 μs, for compositions of (a) 100/0, (b) 80/20, (c) 60/40, (d) 40/60, (e) 20/80, and (f) 0/100.

The contact time study above indicates that 1000 μs is the best contact time for all peaks for homopolymers PBT and PAr and PBT/PAr blends. Hereafter, we chose 1000 μs to be the contact time in the following DD/CP/MAS experiments. In Figure 3, we present the DD/CP/MAS ^{13}C spectra for both quenched homopolymers and PBT/PAr blends. PBT homopolymer is the upper spectrum, and PAr homopolymer is the lower spectrum. For all quenched PBT/PAr blends, the NMR spectra are intermediate between those of PBT and PAr homopolymers, as expected. The peak intensity for each carbon is approximately proportional to the mass fraction of PBT or PAr. Both PBT and PAr resonant peaks appear in the blend spectra, and the chemical shifts of these peaks are the same as those of PBT and PAr homopolymers within experimental error.

NMR spectra of melt-crystallized PBT and PBT/PAr blends are shown in Figure 4. Compared with quenched amorphous samples, most peaks of melt-crystallized PBT and PBT/PAr blends are much sharper, which can be

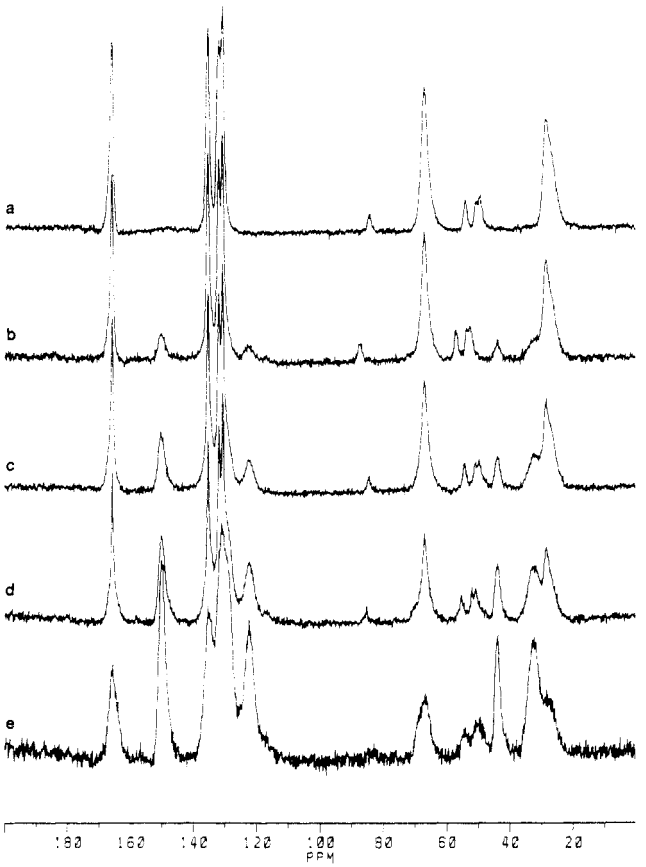

Figure 4. Solid-state ^{13}C NMR spectra for melt-crystallized PBT/PAr blends at a cross-polarization time of 1000 μs, for compositions as listed in Figure 3.

explained by the much more uniform chemical environment of carbons of the PBT crystal phase in both PBT and PBT/PAr blends. These sharper peaks are from the PBT crystalline phase in the blends, while other peaks of the blends have the same full width at half-maximum (fwhm) as those of amorphous PAr. For the 20/80 blend, the melt-crystallized sample shows little difference from that of the quenched amorphous sample, implying very little crystal phase (about 0.01 mass fraction crystallinity) is formed during melt crystallization.[6] This is due to the large PAr content that significantly reduces the ultimate crystallinity of PBT.

The line width of the very sharp peaks (e.g., PBT carbons 1 and 2) seems to decrease systematically from melt-crystallized PBT to 80/20, 60/40, and finally 40/60. For example, the carbonyl peak (PBT 1) located at 163 ppm clearly shows this trend. After subtracting the halo underneath this peak (attributed to the amorphous phase of PBT and PAr), we isolated the contribution from the crystalline PBT phase. The fwhm of this residue peak from crystals is shown to be 1.5 ppm for PBT, 1.1 ppm for 80/20, 0.9 ppm for 60/40, and 0.8 ppm for 40/60. The decrease in fwhm with an increase in the PAr content is due to the crystal size and/or crystal perfection of the samples. A larger crystal size and better crystal perfection would reduce the fwhm, while a smaller crystal size and poor crystal perfection should increase the fwhm by creating a broad distribution of local environments. This qualitative result is consistent with our wide-angle X-ray scattering results, which were used previously to deduce the length scale of PBT crystals in PBT/PAr blends in a *quantitative* way.[6] Although it seems unexpected that the PBT crystal size is larger in the blends than in the PBT homopolymer, this result is due to the difference in crystallization kinetics among the blends. More specifically, blending of PAr with PBT reduces the crystallization

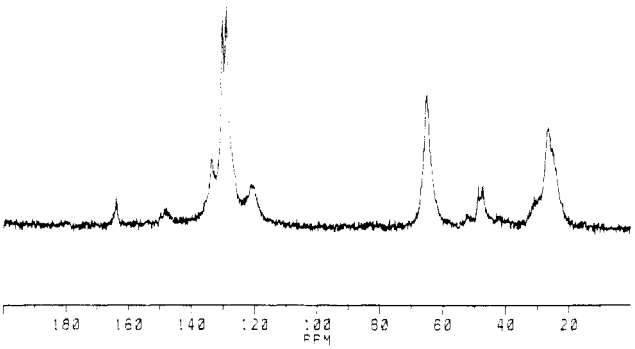

Figure 5. Solid-state ^{13}C NMR spectrum for a melt-crystallized 60/40 PBT/PAr blend at a cross-polarization time equal to 50 μs.

rate of PBT (for the same crystallization temperature) and decreases the equilibrium melting point of PBT.[5] Here we used T_c equal to 200 °C to crystallize all samples, including both PBT and blends. The degree of undercooling (T_m^0-T_c) is reduced significantly as more PAr is added, because T_m^0 decreases with an increase in the PAr fraction.[5] This results in a significant reduction of the crystallization rate in the blends, which is critically dependent on the degree of undercooling, and leads to formation of more perfect crystals.

The most striking observation of this work is that the spectra of crystalline PBT, and PBT/PAr blends with more than 0.40 PBT, reveal for the first time the splitting of protonated aromatic carbons. The two peaks have chemical shifts of 130.2 and 128.8 ppm, showing a 1.4 ppm difference. In Figure 5, we present the solid-state ^{13}C NMR spectrum of a melt-crystallized 60/40 blend at a contact time of 50 μs. We observe a tiny peak at 133 ppm which is from nonprotonated aromatic carbons. In the meantime, two comparably strong peaks located at 130.2 and 128.8 ppm are observed, indicating that the two peaks at 130.2 and 128.8 ppm are from protonated aromatic carbons. This peak splitting has not been observed in previous NMR studies of PBT.[7-10] We suspect that splitting was not observed in prior studies because quenched amorphous or cold-crystallized PBT was used by previous researcher for their studies. Both of these sample types have a lower crystallinity and much poorer crystal perfection compared with our melt-crystallized samples. Failure to observe the protonated carbon peak splitting might also be due to the differences in the instrument resolution.

Peak splitting for either protonated aromatic carbons or aliphatic carbons has been observed in other polymer systems.[18-22] Isotactic polypropylene (i-PP) has been found to exhibit such peak splitting in highly crystallized samples, and this was explained by the conformation sensitive γ-gauche effect.[18,19] Garroway et al.[21] studied ortho-carbon peak splitting in an epoxy polymer. They attributed the splittings to the proximity of the ortho carbons to methyl or methylene protons. The protonated aromatic carbons in poly(phenylene oxide) (PPO) have also shown peak splitting.[20] In a study of poly(*p*-phenylene terephthalamide), English suggested that the ortho carbons in the terephthalic unit exhibited peak splitting because of interaction with amide hydrogens.[22] The absence of peak splitting of the ortho carbons on the aromatic ring in poly(phenylene sulfide) (PPS), which has a similar chemical structure compared with PPO, was explained by Tonelli[23] to be partially due to the longer C–S bond length in PPS compared to the C–O bond length in PPO and is also due to the fast rate of phenyl ring flippng in PPS compared with PPO. The fast flipping rate of phenyl rings in PPS tends to average out the difference between the two different conformations for the protonated aromatic carbons.

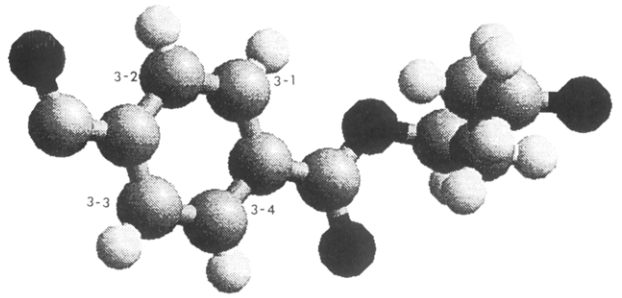

Figure 6. One monomer of PBT in the α phase crystal. The figure was created using Cerius software from Molecular Simulations. Carbons 3–1 and 3–3 exhibit peak splitting from carbons 3–2 and 3–4 due to a slight variation in the local field caused by conformational effects.

The crystal lattice structure of the PBT α phase crystal has been investigated extensively[14–16] and has been shown to possess triclinic crystal structure. We show in Figure 6 one monomer extracted from the α phase crystal lattice, shown with the c-axis horizontal. The disposition of the monomer has been chosen for best viewing of the aromatic carbons and crumpled methylene sequence. The largest atoms are carbons, the smallest atoms are hydrogens, and the black atoms are oxygens. The figure was created using Cerius software from Molecular Simulations. As shown in Figure 6, the four aromatic carbons on one phenyl ring (carbon 3 in Figure 1A) can be separated into two groups, with 3–1 and 3–3 as one group and 3–2 and 3–4 as another group. From symmetry considerations, carbon 3–1 and carbon 3–3 are identical in terms of the local environment in the monomer, and a similar argument holds for carbons 3–2 and 3–4. But, the local field around carbon 3–1 is not equal to that of carbon 3–2, due to the different intramolecular interactions with the neighboring carbonyl. The crystal chain conformation creates small differences in terms of the local field for carbons 3–1 and 3–2, and therefore a small chemical shift difference exists between them. In the quenched noncrystalline PBT this peak splitting is not observed. The difference between the two different conformations in the PBT crystal should diminish as a consequence of increasing the phenyl ring flipping rate, similar to that seen the PPS.[21] High-temperature NMR studies, which can result in fast phenyl ring flipping, are currently being investigated.

4. Conclusion

1. The chemical shifts of carbons in PBT and PAr in the PBT/PAr blends are found to be the same as those of the homopolymers.

2. Contact time studies indicate that the $T_{1\rho}^{H}$ for quenched PBT and PAr are very close in value, at 2.5 and 2.8 ms, respectively. For this reason, miscibility studies based on differences of $T_{1\rho}^{H}$ were not feasible in this experiment.

3. NMR results of melt-crystallized PBT and PBT/PAr blends show that NMR line width decreases as the PAr content increases, indicating larger size crystals appear in the blends compared with that in PBT homopolymer. These results are consistent with our prior studies of the structure of these blends.[5,6]

4. Protonated aromatic carbons of PBT in melt-crystallized PBT and PBT/PAr blends have been observed to exhibit peak splitting for the first time, due to differences of the local environment brought about by chain conformation effects.

Acknowledgment. This research was sponsored by U.S. Army Contract DAAL03-91-G-0132. The authors thank Mark Brillhart for computer modeling of the PBT monomer.

References and Notes

(1) Kimura, M.; Porter, R. S.; Salee, G. *J. Polym. Sci., Polym. Phys. Ed.* **1983**, *21*, 367.
(2) Runt, J. R.; Barron, C. A.; Zhang, X. F.; Kumar, S. K. *Macromol. Commun.* **1991**, *24*, 3466.
(3) Runt, J. P.; Zhang, X.; Miley, D. M.; Gallagher, K. P.; Zhang, A. *Macromolecules* **1992**, *25*, 3902.
(4) Runt, J. P.; Miley, D. M.; Zhang, X.; Gallagher, K. P.; McFeaters, K.; Fishburn, J. *Macromolecules* **1992**, *25*, 1929.
(5) Huo, P.; Cebe, P. *Macromolecules* **1993**, *26*, 589.
(6) Huo, P.; Cebe, P.; Capel, M. *Macromolecules* **1993**, *26*, 4275.
(7) Jelinski, L. W.; Dumais, J. J.; Engel, A. K. *Macromolecules* **1983**, *16*, 403.
(8) Perry, B. C.; Koenig, J. L.; Lando, J. B. *Macromolecules* **1987**, *20*, 422.
(9) Garbow, J. R.; Schaefer, J. *Macromolecules* **1987**, *20*, 819.
(10) Gomez, M. A.; Cozine, M. H.; Tonelli, A. E. *Macromolecules* **1988**, *21*, 388.
(11) Cholli, A. L.; Dumais, J. J.; Engel, A. K.; Jelinski, L. W. *Macromolecules* **1984**, *17*, 2399.
(12) Valero, M.; Iruin, J. J.; Espinosa, E.; Fernandez-Berridi, M. J. *Polym. Commun.* **1990**, *31*, 127.
(13) Huo, P.; Cebe, P. *Polym. Prepr. (Am. Chem. Soc., Div. Polym. Chem.)* **1992**, *30* (1), 140.
(14) Yokouchi, M.; Sakakibara, Y.; Chatani, Y.; Tadokoro, H.; Tanaka, T.; Yoda, K. *Macromolecules* **1976**, *9*, 266.
(15) Mencik, Z. *J. Polym. Sci., Polym. Phys. Ed.* **1975**, *13*, 2173.
(16) Stambaugh, B.; Koenig, J. L.; Lando, J. B. *J. Polym. Sci., Polym. Phys. Ed.* **1979**, *17*, 1053.
(17) Komoroski, S. *High Resolution NMR Spectroscopy of Synthetic Polymers in Bulk*; VCH Publisher, Inc.: Deerfield Beach, FL, 1986.
(18) Bunn, A.; Cudby, M. E. A.; Harris, R. K.; Packer, K. J.; Say, B. J. *Polymer* **1982**, *23*, 694.
(19) Saito, S.; Moteki, Y.; Nakagawa, M.; Morii, F.; Kitamaru, R. *Macromolecules* **1990**, *23*, 3256.
(20) Schaefer, J.; Stejskal, E. O. In *Topics in Carbon-13 NMR Spectroscopy*; Levy, G. C., Ed.; Wiley-Interscience: New York, 1979; Vol. 4, p 283.
(21) Garroway, A. N.; Ritchey, W. M.; Moniz, W. B. *Macromolecules* **1982**, *15*, 1051.
(22) English, A. *J. Polym. Sci., Polym. Phys. Ed.* **1986**, *24*, 805.
(23) Gomez, M.; Tonelli, A. E. *Polymer* **1991**, *32*, 796.